Brazilian Journal
of Chemical
Engineering

ISSN 0104-6632
Printed in Brazil
www.abeq.org.br/bjche

Vol. 29, No. 04, pp. 699 - 712, October - December, 2012

PREPARATION AND CHARACTERIZATION OF SUB-MICRON DISPERSIONS OF SAND IN ETHYLENE GLYCOL-WATER MIXTURE

S. Manikandan, N. Karthikeyan, M. Silambarasan, K. S. Suganthi and K. S. Rajan*

Centre for Nanotechnology & Advanced Biomaterials (CeNTAB), School of Chemical & Biotechnology,
Phone: 91 9790377951, Fax: 91 4362 264120, SASTRA University, Thanjavur – 613401, Tamilnadu, India.
*E-mail: ksrajan@chem.sastra.edu

(Submitted: November 23, 2011 ; Revised: February 24, 2012 ; Accepted: March 23, 2012)

Abstract - Experiments were carried out on the preparation and characterization of dispersions of sand in ethylene glycol-water (50-50%) mixture. The dispersions were prepared by stirred bead milling of 20-30 μm sand (in water) followed by dilution with water and ethylene glycol. The influence of temperature (31-45 °C), particle concentration (< 2 vol %) and ultrasonication on the viscosity of sand-ethylene glycol-water dispersions was studied. The thermal conductivity of dispersions as a function of particle concentration and ultrasonication has also been investigated. Correlations were developed for the prediction of relative viscosity and thermal conductivity ratio of the dispersions. Our results indicate that the sand-ethylene glycol-water dispersions, prepared by stirred bead milling and ultrasonication, have potential as coolants.
Keywords: Stirred bead milling; Sub-micron dispersions; Viscosity; Thermal conductivity; Aggregates; Brownian motion.

INTRODUCTION

Heat exchangers form an essential component in maintaining the energy efficiency of an industry. Some examples include the use of hot flue gas to preheat the solid raw material in cement industries (Rajan *et al*., 2007b; Rajan *et al*., 2008; Rajan *et al*., 2010), heat exchange between hot reaction products and precursors in petrochemical industries, etc. Research in the field of heat transfer is directed towards increasing the heat transfer rate for the same coolant inventory and pumping power or for fixed heat exchanger geometry. One of the methods to improve heat transfer is to utilize liquids with high thermal conductivity. Water, ethylene glycol (EG)-water mixtures, propylene glycol (PG)-water mixtures, Therminol®-VT, Therminol®-55, etc are some of the heat transfer fluids widely used for cooling or heating applications. These heat transfer fluids possess lower thermal conductivities when compared to solids like metals and metal oxides (Wang and Mujumdar, 2007; Wen *et al*., 2009; Palabiyik *et al*., 2011). However these solids cannot be directly used as heating or cooling medium. Following Maxwell's pioneering theoretical work (Maxwell, 1881) several experimental and theoretical studies on the thermal conductivity of suspensions containing solid particles have been carried out (Wang and Mujumdar, 2007). However, the millimeter and micrometer-sized particles settle due to gravity and hence their suspensions cannot be maintained in a static liquid. The properties of nanoparticle dispersions in common coolants have been widely reported and reviewed (Wang *et al*., 2008a; Wang *et al*., 2008b).

The velocity with which micrometer-solid particles settle in a fluid can be estimated by Stoke's law, which predicts the settling velocity to be directly proportional to the square of the particle size and the difference in density between the solid

*To whom correspondence should be addressed

particles and liquid and inversely proportional to the fluid viscosity (Mc Cabe *et al*., 1993). If dispersion of sub-micron particles of density comparable to that of the liquid is made in a slightly viscous liquid, the settling velocity of particles can be reduced. Similarly, Brownian motion, which is effective for smaller particle sizes, retards settling (Sivasankar and Pramod Kumar, 2010). Following the pioneering work of Choi *et al*. (1995), efforts have been made to prepare dispersions of nanoparticles (1-100 nm) in common coolants, leading to nanofluids with higher thermal conductivity than the liquid in which the nanoparticles are dispersed. However, a certain degree of agglomeration takes place when nano-particles are dispersed, leading to a wide hydro-dynamic size distribution (Wen and Ding 2005; He *et al*., 2007; Longo and Zilio 2011; Ghadimi *et al*., 2011).

In the present work, sub-micron dispersions of sand were prepared in an ethylene glycol (50 vol %) - water (50 vol %) mixture through stirred bead milling followed by ultrasonication. The choice of sand is due to its ready availability and its low density. Assuming free settling, the terminal settling velocity of 300 nm sand particles (density ~ 2650 kg/m^3) in ethylene glycol (50 vol %) – water (50 vol %) mixture calculated using Stoke's equation is ~3x10^{-8} m/s. Hence, the time taken for these particles to travel 1 cm through settling in a static EG-water mixture is ~ 92 h. In case of hindered settling without particle agglomeration, the settling velocity would be lower than that corresponding to free settling and hence would require a longer time to settle (McCabe *et al*., 1993). Hence, it is possible to prepare stable dispersions of sub-micron particles in an ethylene glycol-water mixture. Despite containing particles on a nanometer scale, these dispersions are different from nanofluids, which are prepared by dispersing engineered nanoparticles of a specific size and shape. However, these dispersions can also be expected to possess higher thermal conductivity if the colloidal stability can be maintained. The influence of particle concentration and ultrasonication on viscosity and thermal conductivity of sand-ethylene glycol-water dispersions prepared by stirred bead milling were also studied and are reported here.

MATERIALS AND METHODS

Preparation of Sub-Micron Dispersions

The sub-micron suspensions were first prepared by stirred bead milling of properly-ground and sieved river-bed sand with an average particle size of 20-30 μm, in water. The dimensions of the stirred bead mill and the operating conditions are given in Table 1. These conditions were optimized for preparation of sub-micron suspensions in water, after identifying the controlling variables through a literature survey (Pradeep and Pitchumani, 2011; Stenger *et al*., 2005) and experiments. Stirred bead milling was performed for 6 hours with 0.4 mm Yttrium-stabilized Zirconia (YSZ) beads, followed by milling for another 6 hours using 0.2 mm YSZ beads. At the end of 12 hours of milling, about 250 mL of suspension containing 60 g of sand in water was obtained. Various concentrations of sub-micron dispersions were prepared by serial dilution of the sand-water sub-micron suspension with water and then with ethylene glycol, in such a way that the liquid represented an ethylene glycol (50 vol %)-water (50 vol %) mixture. This led to preparation of sub-micron dispersions of sand-ethylene glycol-water containing different volume fractions of sand. To ensure homogeneity, the dispersions were homogenized in a high-shear homogenizer (T25, UltraTurrax, Germany). Two sets of dispersions were prepared – One set of dispersions was characterized after shear homogenization; the other set was subjected to probe ultrasonication for 6 hours before the characterization studies were carried out. This enabled the investigation of the role of ultrasonication in altering the agglomerate size distribution and its influence on transport properties.

Table 1: Specification of the stirred bead mill and operating conditions.

Specification	Value/Material
Material of construction	**Stainless steel**
Diameter of the mill	125 mm
Height of the mill	200 mm
Number of pins (attached to the stirrer)	16 (4 at each axial location; 4 axial locations)
Length of pins	40 mm
Cooling Jacket	Mild steel
Feed concentration (g/mL)	0.12
Ball loading, J (-)	0.8
Stirrer tip velocity (m/s)	9.24

Laser and X-Ray Diffraction

The particle size distributions of dispersions were determined using the laser diffraction technique (Microtrac Bluewave, Japan). Since the measurement was made in liquid, the distribution of hydrodynamic diameters was obtained, which also provides information on the extent of agglomeration of the sub-micron particles dispersed in ethylene glycol-water mixture. The measurement of particle size

distribution through laser diffraction is advantageous on two accounts: (i) ease of the sample preparation procedure; (ii) the state of dispersion is unmodified during sample preparation or analysis.

A small quantity of the dispersion was freeze-dried and analyzed using a Bruker D8 Focus X-ray Diffractometer to identify possible crystalline phases present in sand, apart from the estimation of the minimum crystallite size using Scherrer's equation. The zeta potential was measured using a Zetasizer (Nano-ZS, Malvern Instruments, USA).

Viscosity and Thermal Conductivity Measurements

The viscosity of dispersions and that of the ethylene glycol-water (50 - 50%) mixture was measured using a digital viscometer (LVDV Pro-II, Brookfield Engineering, USA). The viscosity measurements were reproducible within ±0.5 % error. The thermal conductivity of dispersions and that of ethylene glycol-water (50 – 50%) mixture was measured by transient hot-wire technique (KD-2 Pro, Decagon Devices, USA) using a KS-1 probe. Sufficient care was taken to eliminate convection effects. The instrument was able to provide reproducible values of the thermal conductivity of water with a ±1 % error in the temperature range of 31-45 °C. A constant temperature bath (TC-502, Brookfield Engineering, USA) capable of maintaining set temperature within ±0.1 °C, was utilized to maintain the temperature of the samples during the measurement of viscosity and thermal conductivity.

Uncertainty Analysis

The measurements of viscosity and thermal conductivity were repeated thrice to estimate their standard deviation. Relative viscosity and the thermal conductivity ratio were calculated from the viscosities and thermal conductivities of ethylene glycol-water (50 - 50%) and the dispersions. Hence, the uncertainty in the estimation of the relative viscosity ($U_{\mu r}$) and thermal conductivity ratio (U_{kr}) was calculated as follows using methods reported in literature (Rajan *et al*., 2007a):

$$U_{\mu_r} = \pm\left[\left(U_{\mu}\frac{\partial\mu_r}{\partial\mu}\right)^2 + \left(U_{\mu_d}\frac{\partial\mu_r}{\partial\mu_d}\right)^2\right]^{0.5} \quad (1)$$

$$U_{k_r} = \pm\left[\left(U_{k}\frac{\partial k_r}{\partial k}\right)^2 + \left(U_{k_d}\frac{\partial k_r}{\partial k_d}\right)^2\right]^{0.5} \quad (2)$$

At a confidence level of 95%, the ranges of relative viscosity and thermal conductivity ratios are $\mu_r \pm U_{\mu r}$ and $k_r \pm U_{kr}$ respectively.

RESULTS AND DISCUSSION

Particle Size Distribution

The particle size distribution of sub-micron dispersions of sand in the ethylene glycol-water mixture is shown in Figure 1 for both the ultrasonicated and non-ultrasonicated dispersions. In the initial periods of stirred bead milling, a gradual size reduction of micron-sized precursors took place, resulting in a shift of the product size distribution towards lower particle sizes (Fadhel *et al*., 1999). Once the sub-micron particles are formed, attractive forces between particles begin to influence the product size distribution. With finer particles, the attractive forces between the particles are high owing to the larger surface area (Phuoc and Massoudi, 2009) and hence the tendency to agglomerate is also high (Phuoc and Massoudi, 2009). Hence, the size distribution of the dispersion obtained after stirred bead milling is expected to consist of aggregates formed from small particles as well as the relatively large single particles. The product size distribution of the non-sonicated dispersion (Figure 1) has a mode of 243 nm with 28% of the particles/aggregates less than 100 nm. Upon probe sonication for 6 hours, the size distribution of the dispersion (Figure 1) exhibits two modes, one at 86 nm and the other at 204 nm. The shift in the particle size distribution towards lower values due to ultrasonication is also evident from Figure 1. The role of ultrasonication in breaking loose agglomerates of particles has been well established, with the latest reports being those of Garg *et al*. (2009) and Longo and Zilio (2011). However, it is also understood that ultrasonication cannot cause primary particle breakage or reduce the size of primary particles. Hence, we believe that probe sonication resulted in breakage of some of the particle agglomerates, resulting in the two modes. The mass percentage of particles/agglomerates less than 100 nm also increased to 59.3% as a result of probe sonication, apart from the reduction of mass percentage of particles/aggregates larger than 250 nm to about 4%.

The powder X-ray diffractogram of the dried sand sample is shown in Figure 2. The peaks corresponding to 2θ values of 27 ° and 50.5 ° are representative of (011) and (001) faces of quartz. The broad nature of the peaks supports the presence of nanograins in the

milled sample. The minimum crystallite size was calculated to be 45.17 nm from the Scherrer formula, which correlates reasonably well with the smallest particle size measured by the laser diffraction. The zeta potential was found to be -24.8 mV.

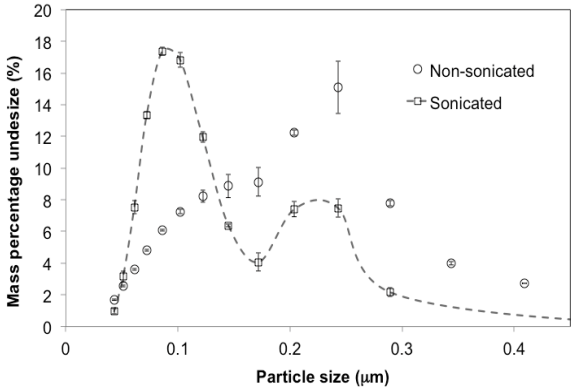

Figure 1: Influence of ultrasonication on the particle size distribution of a sand-ethylene glycol-water dispersion.

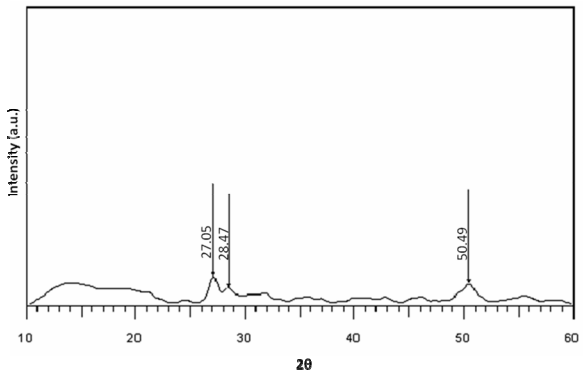

Figure 2: X-ray diffraction pattern of milled powders showing the presence of quartz phase.

Influence of Ultrasonication on Viscosity

The dispersions as well as the ethylene glycol-water mixture exhibited Newtonian characteristics over a shear rate range of 73-245 s^{-1}, for which the accurate measurement of viscosity was possible with the viscometer utilized. The Newtonian characteristics may be attributed to the low concentration of the dispersions employed in the present study.

The influence of probe ultrasonication on the viscosity sand in EG-water dispersions is shown in Figure 3 for different concentrations. It may be observed that the viscosity of the dispersions decreased as a result of ultrasonication, for all concentrations of dispersion. This result can be interpreted along the lines as for nanofluids. Longo and Zilio (2011) observed a difference in viscosity of nanofluids formulated using ultrasonication and those formulated by simple mixing of nanoparticles in water. The higher viscosity of non-sonicated nanofluids was attributed to the presence of aggregates of relatively larger sizes compared to those in the sonicated nanofluids, in spite of the same primary particle size in both the sonicated and non-sonicated nanofluids. The average particle sizes in the sonicated and non-sonicated nanofluids of Longo and Zilio (2011) were 155 nm and 220 nm, respectively. As discussed in the previous section, the non-sonicated sand dispersion contain a higher mass fraction of particle agglomerates compared to those in sonicated dispersions. Accordingly, the average aggregate/particle sizes of the sonicated and non-sonicated sand-EG-water dispersions were 99 nm and 130 nm, respectively. Hence, the reduction of viscosity of the dispersions due to ultrasonication may be attributed to the lower average aggregate/ particle size of sonicated dispersions, though the minimum crystallite size in both the sonicated and non-sonicated dispersions are the same.

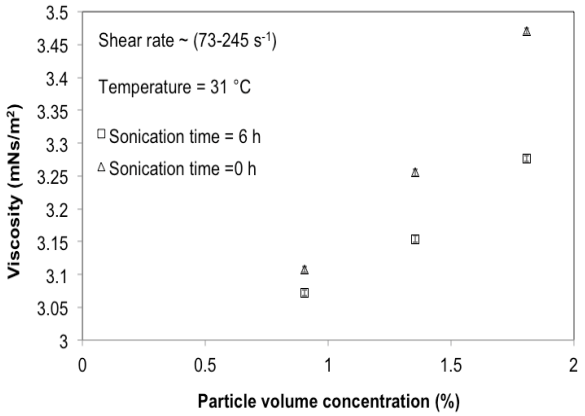

Figure 3: Effect of ultrasonication on the viscosity of sand-ethylene glycol-water dispersions.

Influence of Particle Concentration on Viscosity and Relative Viscosity

The measurement of viscosities of sub-micron dispersions of sand in EG-water mixture was carried out at different particle concentrations (0 – 2 vol %) to elucidate their influence on nanofluid viscosity. Figure 4 shows the influence of particle concentration on the viscosity of sonicated sub-micron dispersions at 31 °C. It is evident that the viscosity of sub-micron dispersions increases with particle concentration. Dispersion of particles in a liquid influences the rheology of liquids by altering the shear stress-shear rate relationship. The influence

of particles is reflected in the higher viscosity values for dispersions compared to that of the EG-water mixture in which they were dispersed. Also, the progressive increase in the viscosity of the dispersion with particle concentration may be attributed to the increase in number of particles in the dispersion (with concentration) which would influence its viscosity.

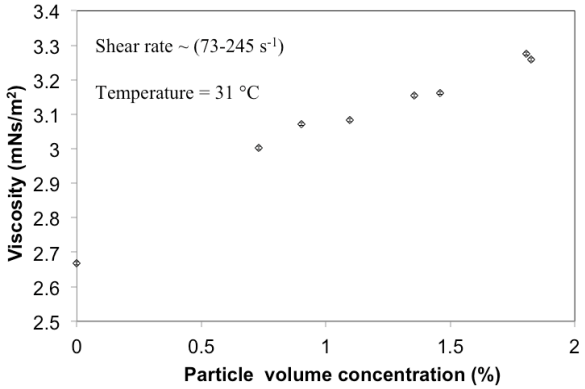

Figure 4: Influence of particle concentration on the viscosity of ultrasonicated sand-ethylene glycol-water dispersions.

Relative viscosity indicates the viscosity of a liquid relative to that of another liquid. It has been widely used to compare the viscosity of polymer solutions with that of the solvent and the viscosity of nanofluids with that of the base fluid (Chen *et al*., 2007). Similarly, relative viscosity may also be defined for sub-micron dispersions as the ratio of the viscosity of the sub-micron dispersions to the viscosity of the base fluid.

Figure 5 shows the influence of particle concentration on the relative viscosity of sand-EG-water dispersions at 31 °C, from which a linear increase in relative viscosity with particle concentration may be observed for both the sonicated and non-sonicated dispersions. Since relative viscosity is directly proportional to the viscosity of the sub-micron dispersion, relative viscosities of non-sonicated suspensions are higher than those of sonicated dispersions. The linear increase of relative viscosity with nanoparticle concentration has been widely observed (Heris *et al*., 2006; Garg *et al*., 2008; Chen *et al*., 2009; Lee *et al*., 2010) when there are no interactions between particles. The sub-micron dispersions reported here are dilute, with particle volume fractions less than 0.02. Hence the distance between the particles or between the particle agglomerates is high, minimizing the particle-particle interactions or aggregate-aggregate interactions, leading to a linear variation of relative viscosity with particle concentration. Though the formation of aggregates itself is a result of particle-particle interactions, they were formed during the preparation of the sub-micron suspension by stirred milling where the particle concentration is relatively high (~ 9 vol %). A certain degree of de-agglomeration was achieved through ultrasonication as discussed in the particle size distribution section.

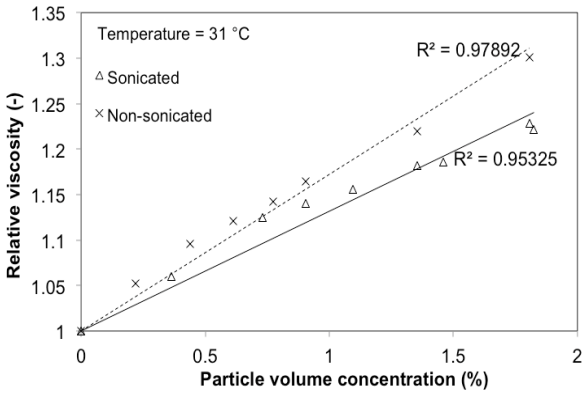

Figure 5: Influence of particle volume concentration on relative viscosity for ultrasonicated and non-sonicated dispersions of sand in the ethylene glycol-water mixture.

The Einstein equation, as cited in Phuoc and Massoudi (2009), relates the relative viscosity (μ_r) with particle concentration (ϕ) via:

$$\mu_r = 1 + 2.5\phi \tag{3}$$

Ghadimi *et al*. (2011) observed that the Einstein equation was applicable to particle volume fractions less than 0.02. Several other equations, like those of Mooney (1951), Brinkman (1952), Krieger and Dougherty (1959), Frankel and Acrivos (1967), Nielson (1970), Lundgren (1972), Brenner & Condiff (1974), and Batchelor (1977) have been proposed for the prediction of relative viscosities of dispersions of nanoparticles in a liquid. All the above equations, except that of Einstein, predict a non-linear variation of the relative viscosity with particle concentration. The relative viscosity-particle concentration relationship for the sub-micron dispersions of the present study is as follows:

For sonicated sand-EG-water dispersions:

$$\mu_r = 1 + 13.1\phi \tag{4}$$

For non-sonicated sand-EG-water dispersions:

$$\mu_r = 1 + 17.2\phi \quad (5)$$

Comparison of Eqs. (4) and (5) with the Einstein equation show that the constants in these equations (13.1 and 17.2) are higher than those proposed by Einstein (2.5), which is applicable for spherical, non-interacting particles in a dilute dispersion (Nguyen *et al*., 2007). When the dispersion contains an appreciable amount of agglomerates, the particle volume fraction (ϕ) may be replaced by aggregate volume fraction (ϕ_a). Chevalier *et al*. (2007) and Chen *et al*. (2007) have proposed modifications of the Kreiger-Dougherty equation, by replacing the particle volume fraction (ϕ) by the aggregate volume fraction (ϕ_a).

Hence, Eqs. (4) and (5) may be rewritten as in the form of Einstein equation with ϕ replaced by ϕ_a:

$$\mu_r = 1 + 2.5\phi_a \quad (6)$$

Chen *et al*. (2009) provided a relationship between ϕ and ϕ_a through the primary particle size (a), the average aggregate size (a_a) and the fractal dimension (D) as follows:

$$\phi_a = \phi\left(\frac{a_a}{a}\right)^{3-D} \quad (7)$$

The particle size distributions show the volume fraction (x_i) of clusters/particles of each size (a_{ai}), which implies that a nanofluid with nanoparticle concentration (ϕ) contains aggregates/particles of several sizes whose volume fractions are (ϕx_i). Accordingly, ϕ_a may be related to particle size distribution as follows:

$$\phi_a = \sum_{i=1}^{n} \phi x_i \left(\frac{a_{ai}}{a}\right)^{3-D} = \phi \sum_{i=1}^{n} x_i \left(\frac{a_{ai}}{a}\right)^{3-D} \quad (8)$$

Substituting Eq. (8) in Eq. (6) gives:

$$\mu_r = 1 + 2.5\phi \sum_{i=1}^{n} x_i \left(\frac{a_{ai}}{a}\right)^{3-D} \quad (9)$$

With the size distribution information obtained from laser diffraction and the minimum crystallite size from the Scherrer formula, Eq. (9) was solved with relative viscosity-particle concentration data to determine 'D' for sonicated and non-sonicated dispersions. Accordingly, 'D' was found to be 1.51 and 1.71 for sonicated and non-sonicated nanofluids, respectively.

Hence, it is clear that the fractal index has decreased as a result of ultrasonication. Higher values of 'D' indicate the presence of dense and compact aggregates, compared to lower values of 'D' indicating loose and open aggregates (Saltiel *et al*., 2004). Hence, probe sonication would have resulted in loosening of dense aggregates. Saltiel *et al*. (2004) observed a reduction in the fractal index with ultrasonication for nanoparticle dispersions in water.

The value of fractal index also throws light on the optimum ultrasonication time or energy required for obtaining lower values of relative viscosity. For two dispersions with identical size distribution, lower relative viscosity will be observed for dispersions that have higher value of D, i.e., the dispersion with dense and compact aggregates, as understandable from Equation (9). For the dispersions of the present study, although reduction in the aggregate size distribution towards lower values as a result of sonication is advantageous for reducing the relative viscosity, this is partly offset by the formation of loose and open aggregates. Hence, the parameters of sonication, including time of sonication, time between successive cycles, etc., must be optimized to produce compact aggregates with a size distribution in the lower range.

Influence of Temperature on Viscosity

The viscosity measurements were carried out at different temperatures between 31 and 45 °C to study the influence of temperature on the viscosity of dispersions. Figure 6 shows the influence of temperature on viscosity of sand-ethylene glycol-water dispersions. It may be observed that the viscosity of the dispersions decreases with temperature. To understand the relative rate at which the viscosity of dispersions and that of the EG-water mixture decrease with temperature, a plot of $\mu^{-1}(d\mu/dT)$ vs T, as shown in Figure 7, was made for all dispersions. It is evident from Figure 7 that the viscosity of the 0.9% dispersion declined more rapidly with temperature, than that of the EG-water mixture or the other dispersions. Hence, the relative viscosity of 0.9% dispersions decreases with temperature, as observed in Figure 8. For other dispersions, the viscosity decrease with temperature is less rapid than that of the EG-water mixture (Figure 7). Hence, the relative viscosity of 1.36% and 1.81% dispersions increases with temperature (Figure 8).

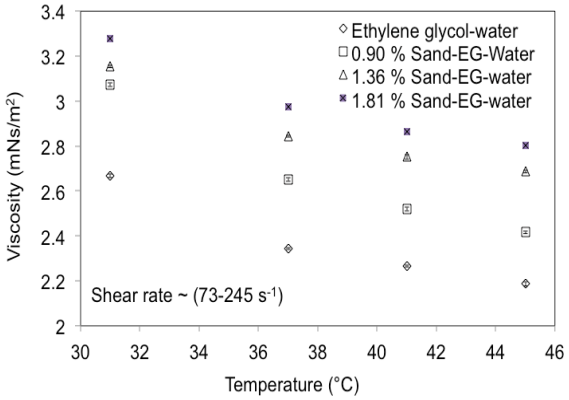

Figure 6: Effect of temperature on the viscosity of sand-ethylene glycol-water dispersions.

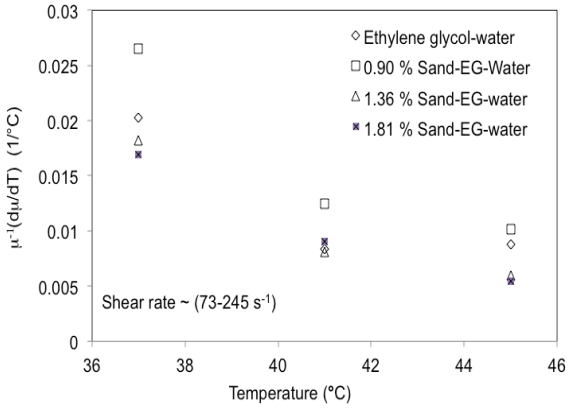

Figure 7: Influence of temperature on the relative rates of decrease of viscosity with temperature for the ethylene glycol-water mixture and sand-ethylene glycol-water dispersions.

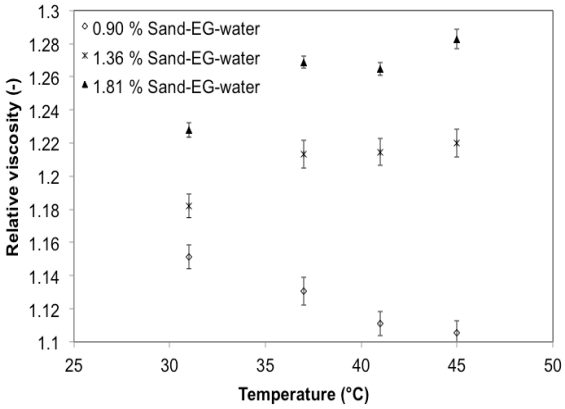

Figure 8: Effect of temperature on the relative viscosity of sub-micron dispersions of sand in ethylene glycol-water mixture.

The literature data on the temperature influence on relative viscosity is scattered, with a majority of them indicating negligible influence of temperature on relative viscosity (Longo and Zilio, 2011; Vajjha *et al*., 2010; Chen *et al*., 2007), while a few others observed an influence of temperature (Nguyen *et al*., 2007; Duangthongsuk and Wongwises, 2009; Lee *et al*., 2011). Interparticle forces, Brownian motion and hydrodynamic forces determine the viscosity of a colloidal dispersion (Genovese *et al*., 2007). At low shear rates, interparticle forces and Brownian motion dominate (Genovese *et al*., 2007). Brownian motion and interparticle forces are temperature-dependent. While higher temperature facilitates Brownian motion, the attractive component of interparticle force decreases with temperature (Lee, 2008). Brownian motion randomizes particle orientation (Bicerano *et al*., 1999), which increases relative viscosity. The increase in relative viscosity with temperature for dispersions with particle concentrations >0.96% of the present study may be attributed to this. At particle concentrations < 0.96%, the decrease in attractive forces with temperature probably dominates over the increase in Brownian motion and hence, for such dispersions, a decrease in relative viscosity with temperature is observed.

Influence of Ultrasonication on the Thermal Conductivity of Dispersions

The influence of probe ultrasonication on the thermal conductivity of sub-micron dispersions of sand in EG-water is shown in Figure 9 for different concentrations at 31 °C. It may be observed that the thermal conductivity of the dispersions increased as a result of ultrasonication, for all concentrations of dispersion. The surface area of dispersed particles is one of the parameters that influences thermal

conductivity of dispersions (Chopkar *et al*., 2008). The total surface area of agglomerates/particles in dispersions is inversely proportional to their size. The increased thermal conductivity for sonicated dispersions may be partly attributed to the higher surface area of the sonicated dispersion due to lower agglomerate/particle sizes. However, the role of particle size in influencing various thermal conductivity enhancement mechanisms is discussed in the next section.

Influence of Particle Concentration on Thermal Conductivity

The influence of particle concentration (< 2 vol %) on thermal conductivity of non-sonicated dispersions at 31 °C is also shown in Figure 9, from which increase in thermal conductivity with particle concentration is evident. As discussed earlier, with an increase in particle concentration, the number of particles in the dispersion increases. Hence, the contribution of particles to the thermal conductivity of the dispersion is greater, leading to increased thermal conductivity of dispersions at higher particle concentrations.

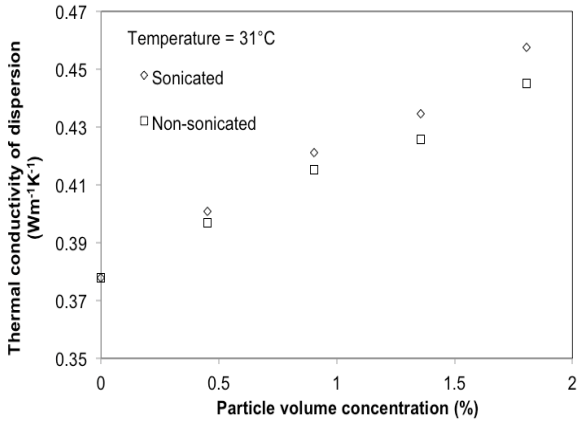

Figure 9: Influence of ultrasonication and particle concentration on the thermal conductivity of sand-ethylene glycol-water dispersions.

The thermal conductivity ratio, defined as the ratio of thermal conductivity of the dispersions to that of the EG-water mixture, is an indicator of enhanced thermal conductivity of the dispersion and hence provides an idea of its possible application for thermal management. The influence of particle concentration on the thermal conductivity ratio at 31 °C is shown in Figure 10 for both the sonicated and non-sonicated dispersions. It is evident from Figure 10 that the thermal conductivity of both the sonicated and non-sonicated dispersions increases linearly with the particle concentration.

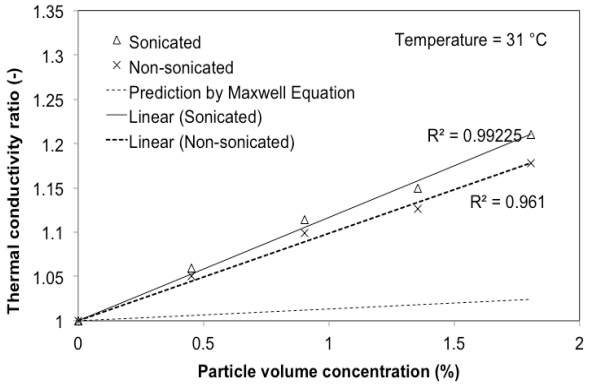

Figure 10: Influence of particle concentration on the thermal conductivity ratio of sonicated and non-sonicated sand-ethylene glycol-water dispersions at 31 °C.

For dilute dispersions of nanoparticles in a liquid (nanofluids), a linear increase in thermal conductivity with particle concentration has been reported (Lee *et al*., 1999; Masuda *et al*., 1993; Vajjha and Das, 2009). Brownian motion, particle clustering, interfacial layering and ballistic transport of energy carriers are considered to be responsible for improved thermal conductivity of nanoparticle dispersions, apart from the contribution from effective medium approximation (Keblinski *et al*., 2002). Brownian motion is predominant for particles/clusters of smaller sizes, as is evident from models for thermal conductivity enhancement incorporating Brownian motion (Xuan *et al*., 2003; Koo and Kleinstreuer, 2004). However, a certain degree of controlled aggregation is considered to be advantageous for obtaining dispersions of higher thermal conductivity by particle clustering (Wen *et al*., 2009). Aggregates of too large sizes would result in poor colloidal stability of the dispersions. Interfacial layering refers to the thin layer of liquid surrounding the particles that is more ordered than the liquid bulk bridging particles and the liquid, with a thermal conductivity greater than that of the liquid (Yu and Choi, 2003). However, interfacial layering is effective only for extremely small particles (Yu and Choi, 2003). The contribution of Brownian motion and particle clustering to the thermal conductivity ratio (k_r) is a function of particle/ aggregate size and may be termed k_a. If $k_{Maxwell}$ is the contribution from Maxwell's effective medium theory for the thermal conductivity ratio, then the total thermal conductivity ratio is given by:

$$k_r = k_{Maxwell} + k_a \quad (10)$$

Within the range of particle concentrations studied here, the contribution from effective medium theory is found to be linear as follows, using the thermal conductivity of sand and the EG-water mixture as 1.3 and 0.378 W/mK respectively:

$$k_{Maxwell} = 1 + 1.3\phi \quad (11)$$

Since the thermal conductivity ratio-particle concentration relationship is linear, the contribution of Brownian motion and particle clustering to the thermal conductivity ratio may be represented as

$$k_{Maxwell} = f\left(\frac{1}{a_a^m}\right)\phi \quad (12)$$

When aggregates of different sizes (a_{ai}) with mass fractions (x_i) are present, Eq. (12) may be modified using the relationship between average aggregate size (a_a) and the aggregate sizes (a_{ai}) as:

$$k_{Maxwell} = f\left(\sum_{i=1}^{n}\frac{x_i}{a_{ai}^m}\right)\phi \quad (13)$$

The analysis of the present data yields the following equation for $k_{Maxwell}$:

$$k_{Maxwell} = 103.593\left(\sum_{i=1}^{n}\frac{x_i}{a_{ai}^{0.5}}\right)\phi \quad (14)$$

Substituting Eq. (11) and Eq. (14) in Eq. (10) gives:

$$k_r = 1 + 1.3\phi + 103.593\left(\sum_{i=1}^{n}\frac{x_i}{a_{ai}^{0.5}}\right)\phi \quad (15)$$

The above equation predicts the thermal conductivity data for non-sonicated and sonicated dispersions of the present study with a correlation coefficient of 0.985 and a standard deviation of 0.0071.The model of Xuan *et al*. (2003) predicts the contribution of Brownian motion and interfacial interactions to thermal conductivity enhancement to be inversely proportional to the square root of the cluster radius. The results of the present study, developed into a correlation (Equation (15)), are in line with the model proposed by Xuan *et al*. (2003).

Sand-Ethylene Glycol-Water Dispersions as Potential Coolant?

The ability of sand-ethylene glycol-water dispersions to function as coolant can be understood from the estimation of the heat transfer coefficient while using them as coolants. The heat transfer coefficient, defined as the ratio of heat flux to the driving force, is a useful parameter in the analysis of heat exchangers. The heat transfer coefficient depends on the transport and thermal properties of the fluid, apart from the flow conditions and geometry. When comparing two coolants with different thermal and transport properties, but under similar flow conditions and geometry, the respective heat transfer coefficients are functions of their viscosities and thermal conductivities as follows:

$$h \alpha k^{a1} \mu^{a2} \quad (16)$$

Equation (16) can be rewritten for sand-EG-water dispersions and the EG-water mixture as follows:

$$h_d \alpha k_d^{a1} \mu_d^{a2} \quad (17)$$

$$h_f \alpha k_f^{a1} \mu_f^{a2} \quad (18)$$

The ratio of the heat transfer coefficient with a sub-micron dispersion as coolant to the heat transfer coefficient with the EG-water mixture as coolant may be called as 'Enhancement factor' (E), a term analogous to enhancement factor used for denoting the enhancement in the mass transfer coefficient while using nanoparticle dispersions over that of the pure liquid alone (Olle *et al*., 2006).

$$E = \frac{h_d}{h_f} = \frac{k_d^{a1}\mu_d^{a2}}{k_f^{a1}\mu_f^{a2}} = k_r^{a1}\mu_r^{a2} \quad (19)$$

Under laminar flow conditions, 'a_1' and 'a_2' are 0.667 and 0 respectively, as is evident from the Seider-Tate and Shah equations cited in Heris *et al*. (2006) and He *et al*. (2007), respectively. Different values of 'a_1' and 'a_2' have been reported for turbulent flows in the literature (Pak and Cho correlation (1998), Xuan and Li, Dittus-Boelter, Gnielinski correlations as cited in Vajjha *et al*. (2010), Vajjha *et al*. (2010) equation). Particle dispersions may enhance the heat transfer coefficient through thermal dispersion effects, apart from their higher thermal conductivity. Hence, the use of correlations developed for conventional fluids to

evaluate particle dispersions represents a conservative approach that provides a minimum enhancement factor achievable through better thermal conductivity alone.

Figure 11 shows the influence of particle concentration of the dispersion on the enhancement factor for laminar and turbulent flows. The values of 'a_1' and 'a_2' for the individual correlation are also given. It is clear that the enhancement ratio increases with particle concentration. However, under turbulent flow conditions, the degree of enhancement is lower when compared to that in laminar flow conditions, where an enhancement factor of 1.14 can be realized with a 1.8% sand-EG-water dispersion. In turbulent flow, the thermal conductivity increase of the dispersion over that of the EG-water mixture is partly offset by its viscosity increase, whereas in laminar flow viscosity does not influence the heat transfer coefficient, as is evident from the value of zero for 'a_2' in the correlations. This indicates the higher suitability of these dispersions for laminar flow conditions.

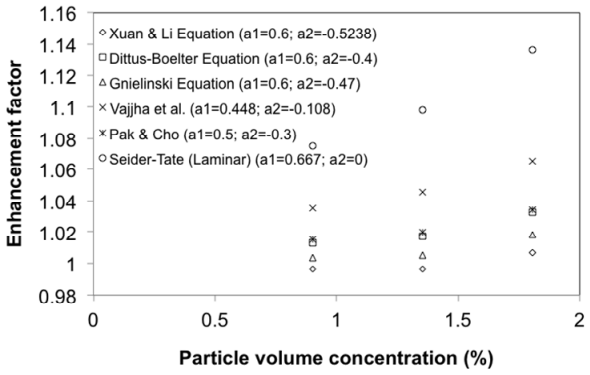

Figure 11: Effect of particle volume concentration on enhancement of the heat transfer coefficient.

Colloidal Stability of Dispersion

To ascertain the colloidal stability of sand-EG-water dispersions, 20 mL of each concentration of dispersion were taken in long, narrow test tubes. Although the colloidal stability can be judged by visually observing them over a time period, a quantitative approach was followed in the present work. A scan of the absorbance of the dispersions in the UV-Visible region showed peak absorbance at a characteristic wavelength (λ_{max}) for the dispersions. Hence, the absorbances of all dispersions were measured at different time periods at the corresponding λ_{max}. Figure 12 shows that the difference in absorbance values measured at different time periods is negligible, which indicates that the dispersion concentrations remained nearly the same, even after 7 days. This highlights the colloidal stability of the dispersions.

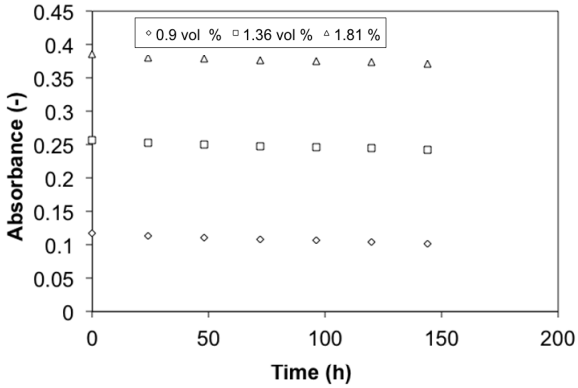

Figure 12: Absorbance at various time periods, highlighting the uniformity of concentration in sonicated sand-ethylene glycol-water dispersions.

Particles in a colloidal dispersion experience various forces, depending upon the interparticle separation, surface charges on the particles and macromolecules grafted on the particle surface (Lee, 2008). Van der Waals, a long-range weak force, is attractive and decays with the increase in interparticle separation. Electrostatic repulsion is a strong, long range-force (Lee, 2008). These two forces are called DLVO forces, which determine the colloidal stability of dispersions in the absence of any macromolecule or polymer grafted on the particle surface. As discussed in the Introduction, the settling velocity of particles of a sub-micron dispersion is too low to allow particle settling in real-time. Brownian motion of the particles brings them closer and, depending upon the relative magnitude of van der Waals and electrostatic repulsion forces, particles may aggregate. In the present study, the dispersions exhibited a zeta potential of -24.8 mV, an indication of higher magnitude of the electrostatic repulsive force. This acts over a long-range and exceeds the magnitude of van der Waals forces, preventing particles from aggregating.

The Brownian velocity may be related to particle size, temperature and dispersion viscosity as follows (Savithiri *et al*., 2011):

$$v_B = \frac{2k_B T}{\pi \mu_d D_p^2} \tag{20}$$

The Brownian velocity for a 300 nm sand particle (maximum size in the present study) in ethylene glycol-water mixture at 31 °C, calculated using Eq. (20), is 1.14×10^{-5} m/s, nearly three-orders of magnitude higher than the settling velocity. Hence, particles would move in this dispersion randomly by Brownian motion compared to downward movement by gravity. This also contributes to stability of the dispersions.

CONCLUSIONS

The following conclusions can be drawn from the present study on the preparation and characterization of sub-micron dispersions of sand in an ethylene glycol-water mixture:

(i) Stirred bead milling followed by ultrasonication is a promising method for preparation of sub-micron dispersions of sand in ethylene glycol-water mixtures with higher thermal conductivity ratio;

(ii) Ultrasonication results in improved transport properties and colloidal stability of the dispersions;

(iii) The thermal conductivity enhancement can be predicted using the contributions from effective-medium theory and Brownian motion;

(iv) These dispersions can enhance the heat transfer coefficient appreciably under laminar flow conditions.

ACKNOWLEDGEMENTS

This work was supported by (i) PG teaching grant No: SR/NM/PG-16/2007 of Nano Mission Council, Department of Science & Technology (DST), India (ii) Grant No: SR/FT/ET-061/2008, DST, India and (iii) Research & Modernization Project #1, SASTRA University, India.

NOMENCLATURE

a	Minimum crystallite or particle size	nm
a_a	Average aggregate size	nm
a_{ai}	Size of aggregates of a class 'i'	nm
a_1	Exponent in Equation (14)	(-)
a_2	Exponent in Equation (14)	(-)
D	Fractal index	(-)
D_p	Particle size in Eq. (20)	m
E	Enhancement in heat transfer coefficient	(-)
h	Heat transfer coefficient	W/m^2K
k	Thermal conductivity	W/mK
k_a	Contribution to the thermal conductivity ratio due to particle size	(-)
k_B	Boltzmann constant (=1.381 x 10^{-23})	J/K
k_r	Thermal conductivity ratio	(-)
$k_{Maxwell}$	Thermal conductivity ratio by the effective medium approximation	(-)
J	Ball loading ~ Volume occupied by beads/volume of feed slurry	(-)
m	Exponent in Equations (10) and (11)	(-)
n	Number of size classes	(-)
T	Temperature	°C or K
x_i	Mass fraction of particles of size a_{ai}	(-)
U	Uncertainty in estimation	(-)
v_B	Brownian velocity	m/s

Greek Symbols

μ	Viscosity of the base fluid	Ns/m^2
μ_r	Relative viscosity	-
ϕ	Particle volume fraction	-
ϕ_a	Particle volume fraction due to aggregates	-
λ_{max}	Wavelength corresponding to maximum absorbance	nm

Subscripts

f	Ethylene glycol-water mixture (base fluid)
d	Dispersion

REFERENCES

Batchelor, G. K., Effect of Brownian-motion on bulk stress in a suspension of spherical-particles. Journal of Fluid Mechanics, 83, no.1, 97-117 (1977).

Bicerano, J., Douglas, J. F. and Brune, D. A., Model for the viscosity of particle dispersions. Polymer Reviews, 39, no. 4, 561-642 (1999).

Brenner, H. and Condiff, D. W., Transport mechanics in systems of orientable particles. IV. Convective transport. Journal of Colloid and Interface Science, 47, no. 1, 199-264 (1974).

Brinkman, H. C., The viscosity of concentrated suspensions and solutions. The Journal of Chemical Physics, 20, 571-581 (1952).

Chen, H., Ding, Y. and Tan, C., Rheological behaviour of nanofluids. New Journal of Physics, 9, 367 (2007).

Chen, H., Witharana, S., Jin, Y., Kim, C. and Ding, Y., Predicting thermal conductivity of liquid suspensions of nanoparticles (nanofluids) based on rheology. Particuology, 7, no. 2, 151-157 (2009).

Chevalier, J., Tillement, O., Ayelaa, F., Rheological properties of nanofluids flowing through microchannels. Appl. Phys. Lett., 91:233103 (2007).

Choi, S. U. S., Enhancing thermal conductivity of fluids with nanoparticles. Developments and applications of non-Newtonian flows. FED-Vol. 231/MD-Vol. 66, 99-105 (1995).

Chopkar, M., Sudarshan, S., Das, P. K. and Manna, I., Effect of particle size on thermal conductivity of nanofluid. Metallurgical and Materials Transactions A, 39, no.7, 1535-1542 (2008).

Duangthongsuk, W. and Wongwises, S., Measurement of temperature-dependent thermal conductivity and viscosity of TiO_2-water Nanofluids. Experimental Thermal and Fluid Science, 33, no. 4, 706-714 (2009).

Fadhel, H. B., Frances, C. and Mamourian, A., Investigations on ultra-fine grinding of titanium dioxide in a stirred media mill. Powder Technology, 105, 362-373 (1999).

Frankel, N. A. and Acrivos, A., On the viscosity of a concentrate suspension of solid spheres. Chemical Engineering Science, 22, no. 6, 847-853 (1967).

Garg, J., Poudel, B., Chiesa, M., Gordon, J. B., Ma, J. J., Wang, J. B., Ren, Z. F., Kang, Y. T., Ohtani, H., Nanda, J., McKinley, G. H. and Chen, G., Enhanced thermal conductivity and viscosity of copper nanoparticles in ethylene glycol nanofluid. Journal of Applied Physics, 103, 074301-306 (2008).

Garg, P., Alvarado, J. L., Marsh, C., Carlson, T. A., Kessler, D. A. and Annamalai, K., An experimental study on the effect of ultrasonication on viscosity and heat transfer performance of multi-wall carbon nanotube-based aqueous nanofluids. International Journal of Heat and Mass Transfer, 52, 5090-5101 (2009).

Genovese, D. B., Lozano, J. E. and Rao, M. A., The rheology of colloidal and noncolloidal food dispersions. Journal of Food Science, 72, no. 2, 11-20 (2007).

Ghadimi, A., Saidur, R. and Metselaar, H. S. C., A review of nanofluid stability properties and characterization in stationary conditions. International Journal of Heat and Mass Transfer, 54, no. 17-18, 4051-4068 (2011).

He, Y., Jin, Y., Chen, H., Ding, Y., Cang, D. and Lu, H., Heat transfer and flow behaviour of aqueous suspensions of TiO_2 nanoparticles (nanofluids) flowing upward through a vertical pipe. International Journal of Heat and Mass Transfer, 50, no. (11-12), 2272-2281 (2007).

Heris, S. Z., Etemad, S. G. and Esfahany, M. N., Experimental investigation of oxide nanofluids laminar flow convective heat transfer. International Communications in Heat and Mass Transfer, 33, no. 4, 529-535 (2006).

Keblinski, P., Phillpot, S. R., Choi, S. U. S. and Eastman, J. A., Mechanisms of heat flow in suspensions of nano-sized particles (nanofluids). International Journal of Heat and Mass Transfer, 45, 855-863 (2002).

Koo, J. and Kleinstreuer, C., A new thermal conductivity model for nanofluids. Journal of Nanoparticles Research, 6, no. 6, 577-588 (2004).

Krieger, I. M. and Dougherty, T. J., A mechanism for non-Newtonian flow in suspensions of rigid spheres. Journal of Rheology, 3, no. 1, 137-152 (1959).

Lee, S., Choi, S. U. S., Li, S. and Eastman, J. A., Measuring thermal conductivity of fluids containing oxide nanoparticles. Journal of Heat Transfer, 121, 280-289 (1999).

Lee, J., Gharagozloo, P. E., Kolade, B., Eaton, J. K. and Goodson, K. E., Nanofluid convection in microtubes. Journal of Heat Transfer, 132, 092401 (2010).

Lee, S. W., Park, S. D., Kang, S., Bang, I. C. and Kim, J. H., Investigation of viscosity and thermal conductivity of SiC nanofluids for heat transfer applications. International Journal of Heat and Mass Transfer, 54, no. (1-3), 433-438 (2011).

Lee, Y. S., Self-Assembly and Nanotechnology: A Force Balance Approach. Wiley, New York, USA (2008).

Longo, G. A. and Zilio, C., Experimental measurement of thermophysical properties of oxide–water nano-fluids down to ice-point. Experimental Thermal and Fluid Science, 35, no. 7, 1313-1324 (2011).

Lundgren, T. S., Slow flow through stationary random beds and suspensions of spheres. Journal of Fluid Mechanics, 51, no. 2, 273-299 (1972).

Masuda, H., Ebata, A., Teramae, K. and Hishinuma, N., Alteration of thermal conductivity and viscosity of liquid by dispersing ultra-fine particles (Dispersions of Al_2O_3, SiO_2 and TiO_2

ultra-fine particles). Netsu Bus-sei (Japan), 7, 227-233 (1993).

Maxwell, J. C., A treatise on Electricity and Magnetism. Clarendon Press, Oxford, UK, Second, Ed. (1881).

McCabe, W. L., Smith, J. C. and Harriott, P., Unit Operations of Chemical Engineering. Fifth, Ed. McGraw-Hill Inc., USA (1993).

Mooney, M., The viscosity of a concentrated suspension of spherical particles. Journal of Colloid Science, 6, no.2, 162-170 (1951).

Nguyen, C. T., Desgranges, F., Roy, G., Galanis, N., Maré, T., Boucher, S., Angue Mintsa, H., Temperature and particle-size dependent viscosity data for water-based nanofluids – Hysteresis phenomenon. Int. J. Heat Fluid Fl., 28, (6):1492-1506 (2007).

Nielsen, L. E., Generalized equation for the elastic moduli of composite materials. Journal of Applied Physics, 41, 4626-4627 (1970).

Olle, B., Bucak, S., Holmes, T. C., Bromberg, L., Hatton, T. A. and Wang, D. I. C., Enhancement of oxygen mass transfer using functionalized magnetic nanoparticles. Industrial & Engineering Chemistry Research, 45, 4355-4363 (2006).

Pak, B. and Cho, Y., Hydrodynamic and heat transfer study of dispersed fluids with submicron metallic oxide particles. Experimental Heat Transfer, 11, no. 2, 151-170 (1998).

Palabiyik, I., Musina, Z., Witharana, S. and Ding, Y., Dispersion stability and thermal conductivity of propylene glycol-based nanofluids. Journal of Nanoparticle Research, 13, (10), 5049-5055 (2011).

Phuoc, T. X. and Massoudi, M., Experimental observations of the effects of shear rates and particle concentration on the viscosity of Fe_2O_3-deionized water nanofluids. International Journal of Thermal Sciences, 48, 1294- 1301 (2009).

Pradeep, P. R. and Pitchumani, B., Effect of operating variables on the production of nanoparticles by stirred media milling. Asia-Pacific Journal of Chemical Engineering, 6, 154-162 (2011).

Rajan, K. S., Dhasandhan, K., Srivastava, S. N. and Pitchumani, B., Experimental study of thermal effectiveness in pneumatic conveying heat exchanger. Applied Thermal Engineering, 27, 1345-1351 (2007a).

Rajan, K S., Dhasandhan, K., Srivastava, S. N. and Pitchumani, B., Studies on gas-solid heat transfer during pneumatic conveying. International Journal of Heat and Mass Transfer, 51, no. 11-12, 2801-2813 (2008).

Rajan, K. S., Pitchumani, B., Srivastava, S. N. and Mohanty, B., Two-dimensional simulation of gas-solid heat transfer in pneumatic conveying. International Journal of Heat and Mass Transfer, 50, 967-976 (2007b).

Rajan, K. S., Srivastava, S. N., Pitchumani, B. and Surendiran, V., Thermal conductance of pneumatic conveying preheater for air-gypsum and air-sand heat transfer. International Journal of Thermal Sciences, 49, no. 1, 182-186 (2010).

Savithiri, S., Pattamatta, A. and Das, S. K., Scaling analysis for the investigation of slip mechanisms in nanofluids. Nanoscale Research Letters, 6, no.1, 471-485 (2011).

Saltiel, C., Chen, Q., Manickavasagam, S., Schadler, L. S., Siegel, R. W. and Menguc, M. P., Identification of the dispersion behavior of surface treated nanoscale powders. Journal of Nanoparticle Research, 6, 35-46 (2004).

Sivasankar, M. and Pramod Kumar, B., Role of nanoparticles in drug delivery system. International Journal of Research in Pharmaceutical and Biomedical Sciences, 1, no. 2 (2010).

Stenger, F., Mende, S., Schwedes, J. and Peukert, W., The influence of suspension properties on the grinding behavior of alumina particles in the submicron size range in stirred media mills. Powder Technology, 156, no. 2-3, 103-110 (2005).

Vajjha, R. S. and Das, D. K., Experimental determination of thermal conductivity of three nanofluids and development of new correlations. International Journal of Heat and Mass Transfer, 52, no. 21-22, 4675-4682 (2009).

Vajjha, R. S., Das, D. K. and Kulkarni, D. P., Development of new correlations for convective heat transfer and friction factor in turbulent regime for nanofluids. International Journal of Heat and Mass Transfer, 53, no. 21-22, 4607-4618 (2010).

Wang, X. and Mujumdar, A. S., Heat transfer characteristics of nanofluids: A review. International Journal of Thermal Sciences, 49, 1-19 (2007).

Wang, X. and Mujumdar, A. S., A review on nanofluids – Part I: Theoretical and numerical investigations. Brazilian Journal of Chemical Engineering, 25, no. 4, 613-630 (2008).

Wang, X. and Mujumdar, A. S., A review on nanofluids – Part II: Experiments and applications. Brazilian Journal of Chemical Engineering, 25, no. 4, 631-648 (2008).

Wen, D. and Ding, Y., Formulation of nanofluids for natural convective heat transfer applications.

International Journal of Heat and Fluid Flow, 26, no. 6, 855-864 (2005).

Wen, D., Lin, G., Vafaei, S. and Zhang, K., Review of nanofluids for heat transfer applications. Particuology, 7, no. 2, 141-150 (2009).

Xuan, Y., Li, Q. and Hu, W., Aggregation structure and thermal conductivity of nanofluids. AICHE Journal, 49, no. 4, 1038-1043 (2003).

Yu, W. and Choi, S. U. S., The role of interfacial layers in the enhanced thermal conductivity of nanofluids: a renovated Maxwell model. Journal of Nanoparticle Research, 5, 167-171 (2003).